

PROGRESS WITH FEL-BASED COHERENT ELECTRON COOLING *

Vladimir N. Litvinenko[#], Ilan Ben Zvi, Michael Blaskiewicz, Yue Hao, Dmitry Kayran, Eduard Pozdeyev, Gang Wang, Brookhaven National Laboratory, Upton, NY 11973, USA
 George I. Bell, David L. Bruhwiler, Andrey Sobol, Tech-X Corp., Boulder, CO 80303, USA
 Oleg A. Shevchenko, N.A. Vinokurov, Budker Institute of Nuclear Physics, Novosibirsk, Russia
 Yaroslav S. Derbenev, TJNAF, Newport News, VA, USA
 Sven Reiche, UCLA, Los Angeles, CA, USA

Abstract

Cooling intense high-energy hadron beams remains a major challenge for accelerator physics. Synchrotron radiation is too feeble, while efficiency of two other cooling methods falls rapidly either at high bunch intensities (i.e. stochastic cooling of protons) or at high energies (i.e. e-cooling). The possibility of coherent electron cooling, based on high-gain FEL and ERL, was presented at last FEL conference [1]. This scheme promises significant increases in luminosities of modern high-energy hadron and electron-hadron colliders, such as LHC and eRHIC. In this paper we report progress made in the past year on the development of this scheme of coherent electron cooling (CeC), results of analytical and numerical evaluation of the concept as well our prediction for LHC and RHIC. We also present layout for proof-of-principle experiment at RHIC using our R&D ERL which is under construction.

Table 1. Estimates for Cooling Time (in hours) for Various Cooling Mechanisms in RHIC and LHC [2].

Collider	Species	Energy, GeV/n	Synchrotron radiation	Electron cooling	Coherent electron cooling
RHIC	Au, ions	40	∞		0.03 <i>Proof-of-Principle</i>
RHIC	Au, ions	100	∞	~ 1	0.015
RHIC	Protons	250	∞	~ 30	0.12
LHC	Pb, ions	2,750	10	$\sim 4 \cdot 10^4$	0.15
LHC	Protons	7,000	13	∞	< 1

The sign ∞ is used to indicate hopelessly long damping times.

INTRODUCTION

While various possibilities of using electron beam instabilities for enhancing the electron cooling were proposed and discussed since early 1980s [3,4], the paper [1] was the first to suggest a specific CeC scheme and its complete evaluation. As shown in Fig.1, this electron cooling technique is based on electrostatic interaction between electrons and hadrons, which is amplified in a high-gain FEL. The main advantage of coherent electron cooling is that it promises very short cooling times, shown in the Table 1, for high-energy hadron colliders such as RHIC and LHC.

The CeC shown in Figs. 1 has three parts: The Modulator, the FEL Amplifier for electron and Longitudinal Dispersion for Hadrons, and the Kicker. In CeC electrons and hadrons should have the same relativistic factor: $\gamma_o = E_e / m_e c^2 = E_h / m_h c^2$. Here we are interested in ultra-relativistic case $\gamma_o \gg 1$ typical of high-energy hadron colliders. With exception of the middle section of the CeC, the processes are easier to describe in the co-moving frame of reference, where the motion of both electrons and hadrons is non-relativistic. Velocity distributions of such beams in the commoving frame are typically anisotropic $\sigma_{v_\perp} \gg \sigma_{v_z}$ (where

$\sigma_{v_\perp}, \sigma_{v_z}$ are RMS values of transverse and longitudinal velocity distributions in electron beam, correspondently). Further in the text we will use this frame of reference for the modulator.

Hadrons can be protons ($Z=1$), antiprotons ($Z=-1$) or ions with $Z \geq 1$. For simplicity we will talk about positively charged hadrons, because the CeC effect is proportional to Z^2 [1].

From the first principles the CeC operation can be described as follows:

- 1) In the **modulator**, the presence of a hadron in the electron beam creates a motion of electron resulting in partial or complete screening of the hadron. Typical time needed for the screening is about of a quarter of the plasma oscillation period in the electron beam, $T = 2\pi / \omega_p$, and the typical size of the local distortion in the electron density is on the order of Debye radii:

$$r_{D_z} = \sigma_{v_z} / \omega_p; \quad r_{D_\perp} = \sigma_{v_\perp} / \omega_p;$$

$$r_{D_\perp} \gg r_{D_z}.$$

- 2) The pancake like local distortion can be (linearly) amplified in a **high-gain FEL**, where it will be also transformed into a wave-packet of the high and low density slices with the period of the FEL wavelength. Meanwhile, hadrons experience a longitudinal delay and **longitudinal dispersion**, where hadrons with higher energies propagated

* This work is supported the U.S. Department of Energy
[#] vl@bnl.gov

slightly faster than those with lower energy. Thus, the arrival time at the kicker will depend on the energy of the hadron.

- 3) The delays of the wave-packet induced by the hadron (and amplified in the FEL) and the hadron itself are arranged in such a way that in the **kicker** (see Fig.1) a hadron with central energy, E_h , will be located at the peak of electron density modulation, where the electrostatic longitudinal field vanishes. In this case, a higher energy hadron will arrive ahead and will be decelerated by the negatively charged slice, while a lower energy hadron will experience acceleration in the kicker.

As the result of this action, the energy spread of the hadrons will be reduced. Further details of the process as well as the description of redistribution of the cooling to transverse degrees of freedom can be found elsewhere [1].

Even though the principles of CeC operation are straightforward, many details of the process should be studied in depth for an exact evaluation of the system. A suite of theoretical and simulation tools should be developed for predicting accurately the performance of realistic CeC systems. Finally, being a novel concept, the

experimental CeC proof-of-principles demonstration is very desirable.

In order to deepen the understanding of the CeC process we established a program of systematic studies of the main processes of CeC.

In the modulator, we plan to study both theoretically and numerically the response, i.e. modification of the distribution function, of a realistic electron beam on a presence of a moving hadron.

In the FEL, we plan to study the dynamics of the evolution of the of the electron beam distribution function and the influence of the electron beam parameters on the process. We also plan to understand the limits to which linear superposition of individual perturbations is applicable in the FEL.

In the dispersion/transport system for hadrons we plan to focus on the design of relatively inexpensive lattices, which allow to accomplish effective 3D cooling.

In the kicker, we plan to study effects of energy spread of electron beam, induced in the FEL, on the evolution of the e-beam modulation and to optimize the kicker lattice.

Finally, we plan to study in detail collective effects in the CeC.

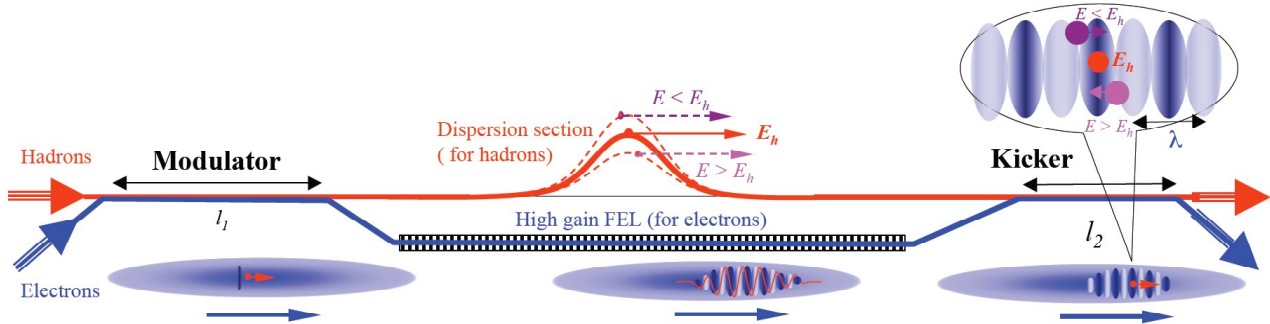


Figure 1: A general schematic of the Coherent Electron Cooler comprising three sections: a **modulator**, an **FEL** plus a **dispersion section**, and a **kicker**. FEL wavelength, λ , in the figure is grossly exaggerated for its visibility.

This paper presents the progress in the studies during last year, which were focused mostly on two systems, which we consider to be most complicated to study: the modulator and the FEL. Because a detailed paper on the FEL response in the CeC is a part of these proceeding [5], here we focus on the modulator.

THE MODULATOR

As we mentioned above, our goal is to develop a complete understanding of the evolution of the response of a realistic electron beam (plasma) in the presence of a hadron with charge Z_h moving with an arbitrary velocity (in co-moving frame $\vec{v}_h = \vec{v}_{||} + \vec{v}_{\perp}$):

$$f(\vec{r}, \vec{v}, t) = \int G(\vec{r}, \vec{r}', \vec{v}, \vec{v}', t | \vec{r}_{io}, \vec{v}_{io}) f(\vec{r}'_{\perp}, \vec{p}', 0) d\vec{r}' d\vec{v}'.$$

Studies of the processes in the modulator proceeded along three main paths: 1) exact analytical evaluation of the plasma response; 2) numerical solutions of the linearized Vlasov equation; 3) digital simulation using the code VORPAL [6,7], which is an ideal numerical tool for investigating both the modulator and the kicker in CeC.

FEL Applications

Table 2: Main electron beam parameters used for the simulation with VOPRAL

E-beam density	n_e [m^{-3}]	$1.6 \cdot 10^{16}$
Plasma frequency	ω_p [sec^{-1}]	7.1410^9
Debye radius (z-dir)	s [m] $\zeta^{1/3}$	8.210^{-6}
Velocity spread	$\sigma_{v_x}, \sigma_{v_z}$, m/sec	$9 \cdot 10^4, 2.710^4$
R	$\sigma_{v_x} / \sigma_{v_z}$	3

Dimensionless equations of motion. In order to make our studies of the modulator concise, we initially focused on defining the set of all important parameters for the simulation of the modulator [8]. One can easily write the Vlasov equation and the Poisson equation for the electron plasma in the presence of a hadron moving along a known trajectory $\vec{r}_h(t) \cong \vec{r}_o + \vec{v}_h t$:

$$\frac{\partial f_e}{\partial t} + \frac{\partial f_e}{\partial \vec{v}} \cdot \frac{e\vec{E}}{m} + \frac{\partial f_e}{\partial \vec{r}} \cdot \vec{v} = 0;$$

$$(\vec{\nabla} \cdot \vec{E}) = 4\pi en_e \left(\frac{Z}{n_e} \delta(\vec{r} - \vec{r}_h(t)) - \int f_e d\vec{v}^3 \right). \quad (1)$$

The most natural way to define all independent variables is to reduce eq. (1) to dimensionless form. The phase of the electron beam plasma oscillation, $\tau = \omega_p t$, is a natural dimensionless time. Velocities can be normalized to σ_{v_z} , while all dimensions can be normalized to the longitudinal Debye length $s = r_{D_z} = \sigma_{v_z} / \omega_p$, which is the smallest scale in the process, giving us:

$$t = \tau / \omega_p; \quad \vec{v} = \vec{v} \sigma_{v_z}; \quad \vec{r} = \vec{\rho} \sigma_{v_z} / \omega_p; \quad \omega_p^2 = \frac{4\pi e^2 n_e}{m}$$

In these variables we get following dimensionless Vlasov equations for the modulator:

$$\frac{\partial f_e}{\partial \tau} + \frac{\partial f_e}{\partial \vec{v}} \cdot \vec{g} + \frac{\partial f_e}{\partial \vec{\rho}} \cdot \vec{v} = 0; \quad \vec{g} = \frac{e\vec{E}}{m\omega_p^2 s}; \quad (2)$$

$$(\vec{\nabla}_n \cdot \vec{g}) = \frac{Z}{s^3 n_e} \delta(\vec{\rho} - \vec{\rho}_i(t)) - \int f_e d\vec{v}^3; \quad \vec{\nabla}_n \equiv \partial_{\vec{\rho}}.$$

Further simplification, i.e. a reduction of the number of variables, comes from specific assumption that we plan to use a round electron beam (i.e. x serves as r!) with a "beer-can" (uniform) transverse distribution with radius a . Thus, we define the following dimensionless parameters of the system:

$$R = \frac{\sigma_{v_x}}{\sigma_{v_z}}; \quad T = \frac{v_{hx}}{\sigma_{v_z}}; \quad L = \frac{v_{hz}}{\sigma_{v_z}}; \quad \xi = \frac{Z}{4\pi n_e R^2 s^3}; \quad (3)$$

$$A = \frac{a}{s}; \quad X = \frac{x_{ho}}{a}; \quad Y = \frac{y_{ho}}{a}.$$

The parameter ξ is proportional to the relative deviation of electron density within the Debye ellipsoidal sphere, and, therefore, represents the degree of the nonlinearity of the Vlasov equation. For typical parameters of the electron beams we plan to use (a sample of beam parameters is given in Ref. [5] in these proceedings), the non-linearity parameter is very low ($\xi \sim 10^{-3}$). This level of relative deviations of electron density is too small for numerical simulations, therefore we use intentionally a slightly higher $\xi \sim 10^{-1} \div 10^{-3}$ for VORPAL simulations (see [9] for more details). A sample of parameters used for VORPAL simulation is given in Table 2.

$$\tilde{n}(\vec{r}, t) = \frac{Z n_o \omega_p^3}{\pi^2 \sigma_{v_x} \sigma_{v_y} \sigma_{v_z}} \int_0^{\omega_p t} \tau \sin \tau \left(\tau^2 + \left(\frac{x - v_{hx} \tau / \omega_p}{r_{Dx}} \right)^2 + \left(\frac{y - v_{hy} \tau / \omega_p}{r_{Dy}} \right)^2 + \left(\frac{z - v_{hz} \tau / \omega_p}{r_{Dz}} \right)^2 \right)^{-2} d\tau; \quad (8)$$

Simple integration of this expression over all space gives, as expected, the same induced charge as eq. (6). Nevertheless, the distribution of the charge depends on the velocity of the ion, the anisotropy of the electron velocity spread and of the functional type of the distribution – the later is demonstrated in Fig.2.

FEL Applications

The simplest case is of infinite cold plasma, where the equation can be reduced to hydrodynamic equation on electron density modulation $\tilde{n} = n - n_o$:

$$\frac{\partial^2 \tilde{n}}{\partial t^2} + \omega_p^2 \tilde{n} = Z \omega_p^2 \delta(\vec{r}_o - \vec{v}_h t), \quad (4)$$

which is easily solvable in the Fourier domain (we use $\vec{r}_o = \mathbf{0}$ further on):

$$n_{\vec{k}} = \frac{Z \omega_p}{(2\pi)^3} \int_0^t dt_1 \sin \omega_p (t - t_1) \cdot \exp(-i(\vec{k} \cdot \vec{v}_h) t). \quad (5)$$

Using (5) it is easy to calculate both the z-density evolution as well as the total induced charge in electron beam:

$$Q_{in} = -e \int \tilde{n} dV = -eZ \cdot (1 - \cos \varphi_p); \quad \varphi_p = \omega_p t. \quad (6)$$

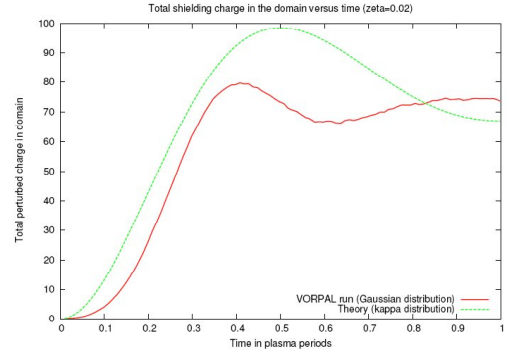


Figure 2: Comparison of the total induced charge within an ellipsoidal sphere of four Debye radii from the Au ion ($Z=79$) obtained from VORPAL simulations (for electron beam with Gaussian energy distribution) with analytical formula [10] for Lorentzian (kappa, $\kappa=2$) distribution.

This result does not change when the electron beam has finite and anisotropic velocity spread. Two of the co-authors of this paper recently found analytical expression for the response on a moving hadron of an infinite electron plasma with anisotropic Lorentzian distribution of velocities [10]:

$$f(\vec{v}) = \frac{n_o}{\pi^2 \sigma_{v_x} \sigma_{v_y} \sigma_{v_z}} \left(1 + \frac{v_x^2}{\sigma_{v_x}^2} + \frac{v_y^2}{\sigma_{v_y}^2} + \frac{v_z^2}{\sigma_{v_z}^2} \right)^{-2}; \quad (7)$$

has following analytical expression (with three Debye radii $r_{Dx} = \sigma_{v_x} / \omega_p$; $r_{Dy} = \sigma_{v_y} / \omega_p$; $r_{Dz} = \sigma_{v_z} / \omega_p$):

$$\tilde{n}(\vec{r}, t) = \frac{Z n_o \omega_p^3}{\pi^2 \sigma_{v_x} \sigma_{v_y} \sigma_{v_z}} \int_0^{\omega_p t} \tau \sin \tau \left(\tau^2 + \left(\frac{x - v_{hx} \tau / \omega_p}{r_{Dx}} \right)^2 + \left(\frac{y - v_{hy} \tau / \omega_p}{r_{Dy}} \right)^2 + \left(\frac{z - v_{hz} \tau / \omega_p}{r_{Dz}} \right)^2 \right)^{-2} d\tau; \quad (8)$$

Presently we are preparing tools to calculate or simulate the response of an infinite electron plasma to the presence of a moving hadron. In some cases we can do it analytically. Fig 3 shows a couple of profiles calculated by VORPAL for Gaussian velocity distribution (see table 2) and using analytical expression [10].

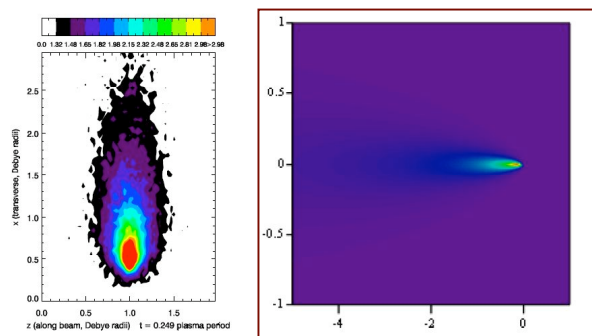


Figure 3: Left figure: A longitudinal cross section of the wake behind a transversely moving gold ion (VORPAL, $T = 1.8$ and $L = 0$, [9]). Right figure- A longitudinal cross section of the wake behind a longitudinally moving gold ion (analytical formula, $T = 0$, $L=10$, see [10] for details). The color is denoting density enhancement taken at about half a plasma period. Coordinates are in units of appropriate Debye radii.

The direct comparison presented in Fig.4 of VORPAL simulations with analytical formula for Lorentzian distribution show reasonable agreement both in the shape of the longitudinal density profile and the value of the induced charge with four Debye radii. The differences, which we suspect are coming from finite grid sizes and finite size of the plasma used in VORPAL simulations, are most noticeable in the beginning of the plasma oscillation.

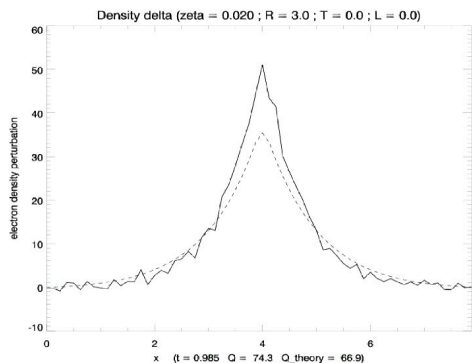


Figure 4: Comparison of longitudinal density profile induced by resting gold ion (in the co-moving frame, Lorentzian distribution in electron beam) calculated by VORPAL (solid line) with analytical formula. Profiles are taken at about half a plasma period. The total charge under the curve is $QV=74.3e$ from VORPAL simulations and $Q_{th}=66.9e$ from the analytical formula (8).

THE FEL

We used 1D FEL theory as well as two 3D FEL codes (RON and Genesis) to find linear time-dependent FEL response, i.e. Green function, on the initial density modulation at its entrance – see [5] for details.

CONCLUSIONS

We developed necessary tools for predicting the response of infinite electron plasma on presence of a

moving ion. These tools, in combination with 1D FEL Green function, allow for a deeper analysis of the CeC processes and for addressing many issues relevant to its performance and potential limitations.

We will continue to refine the tools and to improve their accuracy, as well as study effects of the finite size of electron beam in the modulator and 6D FEL Green function. We are making first steps in the analysis of the kicker and expect to have first result within few weeks.

Finally, we plan to test CeC in a proof-of-principle experiment – shown in Fig.5 - using 20 MeV R&D ERL, which is under construction at BNL, installed in one of available interaction regions at RHIC.

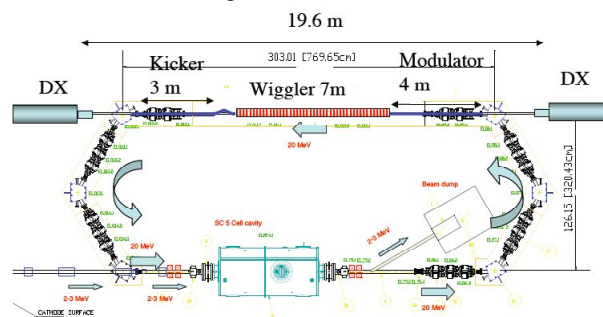


Figure 5: Layout of CeC PoP at RHIC.

REFERENCES

- [1] V.N. Litvinenko, Y.S. Derbenev, Proc. of 29th International FEL Conference, Novosibirsk, Russia, August 27-31, 2007, p.268, <http://accelconf.web.cern.ch/accelconf/f07>
- [2] V.N. Litvinenko, Y.S. Derbenev, EPAC'08 Proc., 2008, p.2548, <http://accelconf.web.cern.ch/AccelConf/e08>
- [3] Ya. S. Derbenev, Proc. of 7th All-Union Conference on Charged Particle Accelerators, 14-16 October 1980, Dubna, USSR, p. 269 (in Russian);
- [4] Ya. Derbenev, AIP Conf. Proc. No. 253, p.103 (1992)
- [5] HIGH GAIN FEL AMPLIFICATION OF CHARGE MODULATION CAUSED BY A HADRON. V.N. Litvinenko et al., these proceedings
- [6] C. Nieter, J.R. Cary, J. Comp. Phys. **196** (2004) 448.
- [7] P. Messmer, D.L. Bruhwiler, Comp. Phys. Comm. **164** (2004), p. 118.
- [8] Dimension-less equations for warm plasma, V.N. Litvinenko, Internal Note, C-AD, BNL, November 26, 2007
- [9] VORPAL Simulations Relevant to Coherent Electron Cooling, G.I. Bell et al, EPAC'08 Proc., 2008, THPC085, <http://accelconf.web.cern.ch/AccelConf/e08>
- [10] Gang Wang and Michael Blaskiewicz, Phys Rev E, volume **78**, 026413 (2008)